english

CSMA 2019
14ème Colloque National en Calcul des Structures
13-17 Mai 2019, Presqu'île de Giens (Var)

Reconstruction of blood flows from Doppler images

F. Galarce[1], J.F. Gerbeau[1], D. Lombardi[1],
O. Mula[2]

[1] *Faculté des Sciences de Sorbonne Université, Centre de Recherche INRIA de Paris and Laboratoire Jacques-Louis Lions, France*
[2] *Université Paris-Dauphine, PSL Research University, CNRS, UMR 7534, CEREMADE, 75016 Paris, France*

Abstract — We address the problem of reconstructing a three dimensional velocity field in a human blood vessel using Doppler ultrasound images. For this, we propose to combine the Doppler measurements with realistic Navier-Stokes models and apply the general state estimation technique introduced in [1]. The method requires finding a reduced basis of the model and a good modeling of the sensor response. In this note, we report preliminary results where we explore the reconstruction quality when we use Principal Component Analysis for the model reduction and model Doppler measurements as bi-dimensional mappings of the velocity over the plane in which the ultrasound probe is pointed to.
Keywords — Flow reconstruction, Inverse problems, Doppler ultrasound, State Estimation, Model Reduction.

1 Optimal reconstruction algorithm

We consider the following state estimation problem: from a set of Doppler ultrasound images, build a reconstruction of the three-dimensional velocity field u in a human blood vessel represented by a domain $\Omega \subset \mathbb{R}^3$. The velocity u will be seen as a function u living in a Hilbert space $\mathcal{H}$ with inner product $\langle \cdot, \cdot \rangle$ and norm $\|\cdot\|$. The reconstruction strategy that we propose is based on the assumption that we know a Partial Differential Equation that models accurately the underlying hemodynamics of the process. However, since we only have access to the Doppler measurements, the appropriate parameters of the PDE are unknown and the problem does not resort to simply solving the PDE. One possibility to do the reconstruction would be to solve a classical inverse problem and find the set of parameters to reconstruct with the associated PDE solution. However, this approach has a high computational cost and cannot be used for online reconstruction. In addition, the reconstruction will always have an intrinsic modelling error that cannot be overcome. An alternative approach yielding an online reconstruction methodology that can overcome to some extend the model error is the following.

We consider the manifold $\mathcal{M} \subset \mathcal{H}$ of solutions of the parametrized PDE model, that is,

$$\mathcal{M} = \{f \in \mathcal{H};\ \mathcal{B}(f;\alpha) = 0\}$$

where $\mathcal{B}$ is the PDE model and $\alpha \in \mathbb{R}^p$ is the vector of parameters ranging in a set $\mathcal{P} \subset \mathcal{R}^p$. Furthermore, we consider a low-dimensional linear space V_n that approximates $\mathcal{M}$ up to a certain accuracy ε_n:

$$\max_{f\in\mathcal{M}} dist(f, V_n) \leq \varepsilon_n$$

We assume that u belongs to the cylinder

$$\mathcal{K} := \{f \in \mathcal{H} : dist(f, V_n) \leq \varepsilon_n\}.$$

Note that this assumption implies that the reduced model approximates u with accuracy ε_n but we do not assume that u belongs to the manifold of solutions $\mathcal{M}$. This detail will become important further on to understand why the method overcomes the model error to some extend.

Regarding the Doppler velocity measurements, we model them as m values $\{l_i(u)\}_{i=1}^m$, where each l_i is a linear functional living in the dual of $\mathcal{H}$ that mimics the action of the action of the sensing device. We defer further explanation on this modeling to the next section and introduce here the space of observations W_m:

$$W_m = span\{\omega_1, \omega_2, \ldots, \omega_m\},$$

where the $\{\omega_i\}_{i=1}^m$ are the Riesz representers of the measures. Assuming that the m linear functionals are linearly independent, the $\{\omega_i\}_{i=1}^m$ are also linearly independent and W_m is of dimension m. As a result, having the vector of measures $l = \{l_i(u)\}_{i=1}^m \in \mathbb{R}^m$ is equivalent to having the orthogonal projection of u into W_m. Therefore, if we summarize the information coming from the measurements and the model, the problem is to

$$\text{Find an approximation } u^* \text{ to } u \text{ given } \omega = P_{W_m} u \text{ and that } u \in \mathcal{K}.$$

In practice, we will have $u \in \mathbb{R}^{\mathcal{N}}$. Let us consider an orthogonal basis $\{\phi\}_i^n$ for V_n and let us arrange it in the columns of a matrix $\Phi \in \mathbb{R}^{\mathcal{N}\times n}$. Also, let us arrange the Riesz representers into the columns of a matrix $W \in \mathbb{R}^{\mathcal{N}\times m}$, which is going to be called the *measure operator*.

The reconstructed field u^* will be the one such that its projection on the orthogonal complement of V_n, i.e., $P_{V_n^\perp} u = (I - \Phi\Phi^T)u$, is minimized:

$$u^* = \arg\inf_{u \in V_n} \frac{1}{2} \|P_{V_n^\perp} u\|^2$$
$$\text{s.t. } W^T u = l$$

This methodology was originally proposed in [1] and a detailed analysis was given in [2]. In particular, it has been proven that the reconstruction with u^* is the best possible reconstruction for the problem (P). It has also been shown that the error in approximating u has the following bound:

$$\|u - u^*\| \leq \frac{1}{\beta(V_n, W_m)} dist(u, V_n \oplus V_n^\perp \cap W_m)$$

where,

$$\beta(V_n, W_m) = \min_{v \in V_n} \frac{\|P_{W_m} v\|}{\|v\|}.$$

The reconstruction is well posed provided that $\beta(V_n, W_m) > 0$, which is an assumption that we make in the following (one can actually realize that this requirement is very mild in realistic cases of application, see, e.g., [3]).

Note that if $m > n$, the error $\|u - u^*\| < \beta(V_n, W_m)^{-1}\varepsilon_n$ and the inequality is strict due to the fact that $V_n^\perp \cap W_m \neq \{0\}$. This shows that the approach corrects to some extend the model error.

2 Doppler measures

In this section, we detail how we model action of the Doppler sensing devices with linear functionals l_i. The Doppler ultrasound images are obtained by using a transducer as the one in figure 1, that estimate the velocity of groups of red blood cells in the vessel by comparing a sequence of ultrasound waves in time (see for example the algorithm shown in [4]).

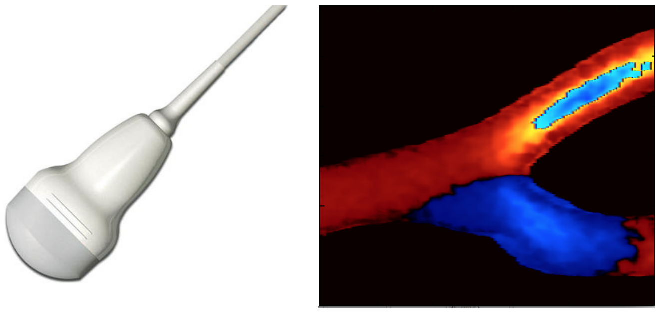

(a) Transducer for ultrasound image acquisition. (b) Typical color flow mapping

Figure 1: Ultrasound device and color flow image.

In classical velocity estimation, what is obtained is a two dimensional mapping of an averaged velocity component in the direction of the ultrasound beam over *sample volumes*, a set of cubic sub-domains (a.k.a. voxels) of the geometry: $\{\Omega_i\}_{i=1}^m$, with $\Omega_i \subset \Omega$. This is,

$$l_i(u) = \int_{\Omega_i} (u) \cdot n \, d\Omega_i$$

Hence, for each image (or measure), we will say that we have a set of m *sub-measures*. Nevertheless, when no misunderstanding can arise, the word sub-measure will be replaced for the word *measure*.

From the fact that all the sample volumes are disjoint sets, it follows that the Riesz representers of the measures are orthogonal to each other. Therefore

$$\omega = P_{W_m} u = \sum_{i=1}^{m} \langle \omega_i, u \rangle \omega_i = \sum_{i=1}^{m} l_i \omega.$$

By inspection of 2 we can see that the Riesz representers are $\omega_i = \chi_i n_i$, where χ_i is a function valued 1 inside Ω_i and 0 outside, and n_i a vector pointing towards the direction of the ultrasound beam.

3 Numerical Example

We have tested the algorithm in a carotid bifurcation geometry (see figure 2), where the numerical resolution of the in-compressible and Newtonian Navier-Stokes equations is performed varying 5 parameters of the flow in order to build the dictionary. In total, the dictionary contains 300 simulations. The numerical solution of the governing laws is done with finite elements (we omit further details on the solver for lack of space).

Let p be the pressure field and u the velocity field. The Navier-Stokes equations for a domain Ω reads

$$\begin{cases} \rho \dfrac{\partial u}{\partial t} + \rho u \nabla u - \mu \Delta u + \nabla p = 0 \text{ in } \Omega \\ \nabla \cdot u = 0 \text{ in } \Omega, \end{cases}$$

where ρ is the density of the flow and μ its viscocity.

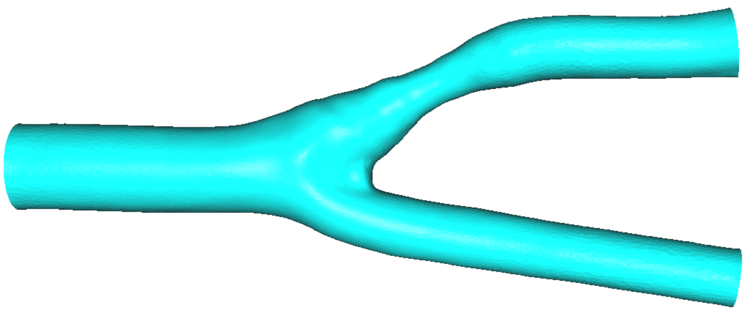

Figure 2: Geometry for the simulations. Note the presence of a small stenosis upstream the bifurcation.

An example of output of the algorithm is given in figure 3. Some statistics for the $L^2(\Omega)$ error are given in the figure 4. We see that we achieve an accuracy of around 10^{-3} with an appropriate choice of n. Further details and results will be given in the forthcoming article [5].

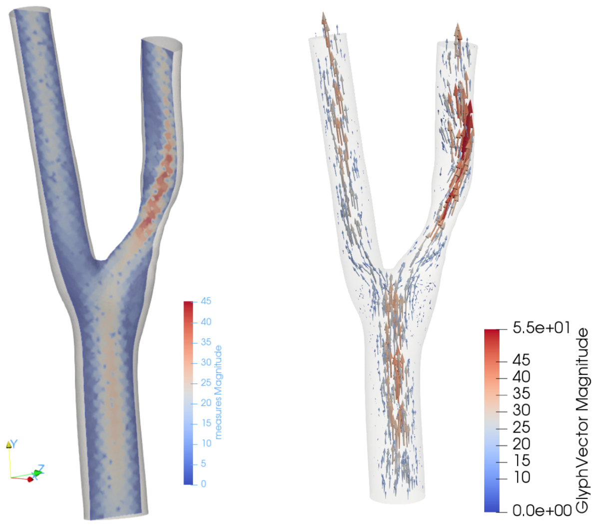

(a) Synthetic measures (b) Reconstructed field

Figure 3: Example for the reconstruction in the common carotid.

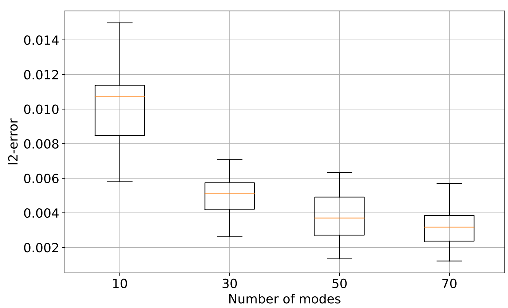

Figure 4: Error vs the dimension of V_n.

References

[1] Y. Maday, A. T. Patera, J. D. Penn, and M. Yano. A parameterized-background data-weak ap- proach to variational data assimilation: formulation, analysis, and application to acoustics. *International Journal for Numerical Methods in Engineering*, 2015.

[2] Peter Binev, Albert Cohen, Wolfgang Dahmen, Ronald DeVore, Guergana Petrova, and Przemyslaw Wojtaszczyk. Data assimilation in reduced modeling. *Society for Industrial and Applied Mathematics and American Statistical Association*, 2017.

[3] P. Binev, A. Cohen, O. Mula, and J. Nichols. Greedy algorithms for optimal measurements selection in state estimation using reduced models. *SIAM/ASA Journal on Uncertainty Quantification*, 6(3):1101–1126, 2018.

[4] Chihiro Kasai, Koroku Namekawa, Akira Koyano, and Ryiozo Omoto. Real-time two-dimensional blood flow imaging using an autocorrelation technique. *IEEE transactions on sonics and ultrasonics*, 1985.

[5] F. Galarce, D. Lombardi, J.-F. Gerbeau, and O. Mula. Reconstruction of blood flows from doppler images and data-driven reduced models. *In progress*, 2019.